

## 2D MATERIALS FOR SUSTAINABLE ENERGY; PHOTOCATALYTIC AND PHOTOVOLTAIC PROPERTIES

Khursheed Ahmed<sup>1</sup>, Rashid Awan<sup>\*2</sup>, Mirza Nauman Ashraf<sup>3</sup>, Quratulain Tariq<sup>4</sup>,  
Shah Wali Ullah<sup>5</sup>

<sup>1</sup>Department of Chemistry, University of Education, Lahore, Pakistan.

<sup>2</sup>Centre of Excellence in Solid State Physics, University of the Punjab, Lahore, Pakistan.

<sup>3</sup>Chemical Department, School of Chemical and Materials Engineering (SCME), NUST, Islamabad, Pakistan.

<sup>4</sup>Institute of physics, The Islamia University of Bahawalpur 63100, Punjab, Pakistan

<sup>5</sup>Dept: Advanced Functional Materials (AFM) Laboratory, Engineering Physics Department, Institute Technology Bandung.

<sup>1</sup>khursheed3626@gmail.com, <sup>2</sup>rashidawan1996@gmail.com, <sup>3</sup>mirza.nauman.ashraf@gmail.com,  
<sup>4</sup>quratulaintariq818@gmail.com, <sup>5</sup>33323751@mahasiswa.itb.ac.id

DOI: <https://doi.org/10.5281/zenodo.17556157>

### Keywords

2D materials; sustainable energy; photocatalysis; photovoltaics; transition-metal dichalcogenides; MXenes; defect engineering; perovskite solar cells

### Article History

Received: 16 September 2025

Accepted: 26 October 2025

Published: 07 November 2025

Copyright @Author

Corresponding Author: \*  
Rashid Awan

### Abstract

Two-dimensional (2D) materials have emerged as promising candidates for advancing sustainable energy technologies owing to their exceptional optical, electronic, and catalytic properties. Their atomically thin structures provide high surface area, tunable band gaps, and strong light-matter interactions, which are highly advantageous for solar-driven energy conversion. In this study, we investigate the photocatalytic and photovoltaic properties of representative 2D materials, including transition-metal dichalcogenides (TMDs), graphitic carbon nitride (g-C<sub>3</sub>N<sub>4</sub>), and MXenes, with emphasis on their structural-functional correlations. Photocatalytic analysis reveals that defect engineering, phase modulation, and heterostructure design significantly enhance charge separation and surface reaction kinetics, resulting in improved performance in hydrogen evolution and carbon dioxide reduction under visible-light irradiation. Photovoltaic evaluation demonstrates that 2D layers can function both as active light absorbers and as interfacial modifiers in perovskite and silicon solar cells, where they effectively suppress non-radiative recombination, improve carrier extraction, and enhance long-term stability. We report that device integration of 2D materials leads to measurable improvements in open-circuit voltage, fill factor, and overall power conversion efficiency. Moreover, the ability to engineer van der Waals heterostructures offers opportunities to construct ultrathin and flexible photovoltaic architectures. Collectively, our findings provide mechanistic insight into the role of atomic structure, defects, and interfacial engineering in dictating energy conversion efficiency. This work establishes a framework for rational design of 2D materials in both photocatalytic and photovoltaic systems, advancing their potential toward scalable applications in clean and renewable energy technologies.

### Introduction

The transition to sustainable and renewable energy sources is a defining challenge of the twenty-first century. Growing global energy demand, depletion of fossil fuel reserves, and

environmental degradation caused by greenhouse gas emissions have necessitated the development of advanced technologies for clean energy production. Solar energy, due to its abundance and universality, is one of the most

promising renewable resources. However, efficient harnessing of solar energy requires breakthroughs in both photocatalytic systems, which drive solar-to-fuel conversion, and photovoltaic systems, which directly convert sunlight into electricity (Zhang et al., 2020).

Two-dimensional (2D) materials have emerged as revolutionary candidates in this domain due to their atomic-scale thickness, tunable band structures, large surface-to-volume ratios, and exceptional light-matter interactions. These properties directly address fundamental bottlenecks in conventional bulk semiconductors, such as limited visible-light absorption, rapid charge carrier recombination, and photocorrosion (Geim & Grigorieva, 2013; Wang et al., 2012). Furthermore, 2D architectures allow for the construction of van der Waals heterostructures with atomically clean interfaces, enabling precise band alignment and efficient charge separation (Novoselov et al., 2016).

A wide variety of 2D materials have been explored for energy conversion. Transition-metal dichalcogenides (TMDs) such as MoS<sub>2</sub> and WS<sub>2</sub> show layer-dependent band gaps and catalytically active edge sites, making them efficient hydrogen evolution catalysts (Jaramillo et al., 2007). Graphitic carbon nitride (g-C<sub>3</sub>N<sub>4</sub>) is a metal-free polymeric semiconductor capable of visible-light photocatalysis, which can be further enhanced by doping and heterojunction engineering (Wang et al., 2009). MXenes and black phosphorus have been employed as conductive charge extraction layers and broadband absorbers, respectively, demonstrating their versatility in both photocatalysis and photovoltaics (Naguib et al., 2011).

Interestingly, progress in nanomaterials and nano-enabled agriculture provides useful parallels for energy research. For example, green-synthesized iron oxide and zinc oxide nanoparticles have been shown to enhance plant physiological performance and nutrient uptake by improving charge transfer processes at the biological interface (Ahmad et al., 2024; Ahmad et al., 2024). Such findings highlight the importance of defect engineering and surface chemistry principles that are equally critical for optimizing 2D materials in photocatalytic and

photovoltaic applications. Similarly, biofortification strategies using nano-enabled approaches (Ahmad et al., 2024) echo the scalability challenges seen in solar energy research, where uniform synthesis and stability of active nanomaterials remain key barriers to industrial adoption.

Beyond synthesis, computational modeling has become indispensable for predicting the structural and electronic properties of new functional materials. Recent bioinformatics studies of gene expression patterns (Rauf et al., 2024) illustrate the power of computational analysis in identifying performance-limiting pathways, an approach increasingly applied to 2D energy materials through density functional theory (DFT) simulations and machine learning. Moreover, sustainable soil amendments and biogenic strategies for crop protection (Sohail et al., 2025) parallel the push toward eco-friendly material processing and lifecycle assessment in solar technologies. These cross-disciplinary insights underscore how sustainable innovation in agriculture, biology, and energy systems is deeply interconnected.

In photovoltaics, 2D materials have been successfully integrated into perovskite and silicon solar cells, functioning as passivation layers, transport interfaces, and transparent electrodes. Their incorporation improves open-circuit voltage, enhances carrier mobility, and mitigates environmental degradation, thereby extending device lifetime (Cao et al., 2015; Mak & Shan, 2016). Moreover, all-2D heterostructure photovoltaics, though at an early stage, showcase unprecedented potential for ultrathin, flexible, and lightweight solar devices. Despite these advances, challenges remain. Scalable synthesis of defect-controlled, environmentally stable 2D layers is not yet industrially feasible. Interfacial quality and long-term durability under operational conditions also hinder device commercialization (Chhowalla et al., 2016). Thus, a deeper mechanistic understanding of how atomic-level features—such as vacancy engineering, phase control, and heterostructure design influence photocatalytic and photovoltaic performance is required.

This paper aims to critically investigate the photocatalytic and photovoltaic properties of 2D

materials, emphasizing their structure function relationships and their role in advancing sustainable energy technologies. By combining insights from nanomaterials research, computational modeling, and cross-disciplinary sustainability studies, this work provides a framework for rational design strategies that can accelerate the deployment of 2D materials in scalable renewable energy systems.

## Methodology

### Materials Synthesis and Preparation

#### Synthesis of 2D Materials

A range of two-dimensional (2D) materials were synthesized, including transition-metal dichalcogenides (TMDs), graphitic carbon nitride ( $g\text{-C}_3\text{N}_4$ ), and MXenes. TMDs such as  $\text{MoS}_2$  and  $\text{WS}_2$  were prepared using a chemical vapor deposition (CVD) process, ensuring control over thickness and crystallinity (Wang et al., 2012).  $g\text{-C}_3\text{N}_4$  was synthesized by thermal polymerization of melamine at 550 °C in a muffle furnace, followed by exfoliation to obtain nanosheets with higher surface area (Wang et al., 2009). MXenes ( $\text{Ti}_3\text{C}_2\text{T}_x$ ) were prepared by selective etching of the Al layer from  $\text{Ti}_3\text{AlC}_2$  MAX phases using a LiF/HCl mixture, followed by delamination via sonication (Naguib et al., 2011).

#### Defect and Heterostructure Engineering

Defect engineering was carried out through controlled annealing in reducing ( $\text{H}_2/\text{Ar}$ ) and oxidizing ( $\text{O}_2$ ) environments to generate vacancy-rich structures. Heterostructures such as  $\text{MoS}_2/g\text{-C}_3\text{N}_4$  and  $\text{MoS}_2/\text{MXene}$  were fabricated using layer-by-layer transfer techniques, enabling clean van der Waals interfaces (Geim & Grigorieva, 2013).

#### Material Characterization

Structural, morphological, and chemical analyses were conducted to confirm the formation of 2D nanosheets. X-ray diffraction (XRD) and Raman spectroscopy were used to determine crystallographic phases and layer-dependent vibrational modes (Mak & Shan, 2016). Transmission electron microscopy (TEM) and atomic force microscopy (AFM) provided nanoscale structural resolution and thickness confirmation. Surface chemistry and defect

states were analyzed using X-ray photoelectron spectroscopy (XPS). Optical properties were examined via UV-Vis absorption spectroscopy and photoluminescence (PL) measurements.

#### Photocatalytic Activity Evaluation

Photocatalytic hydrogen evolution reactions (HER) were tested in a quartz reactor under AM 1.5G simulated sunlight. The catalyst suspension was prepared in aqueous solution containing a sacrificial electron donor such as methanol. Hydrogen evolution was quantified by gas chromatography (GC) equipped with a thermal conductivity detector (TCD). The apparent quantum yield (AQY) was calculated at specific wavelengths to determine efficiency (Zhang et al., 2020).

For  $\text{CO}_2$  reduction, a sealed photoreactor with  $\text{CO}_2$ -saturated aqueous electrolyte was employed. Product distribution, including  $\text{CO}$ ,  $\text{CH}_4$ , and  $\text{HCOOH}$ , was analyzed using gas chromatography mass spectrometry (GC-MS). Photocatalytic oxygen evolution reaction (OER) activity was evaluated using a sodium persulfate solution as electron scavenger, with evolved  $\text{O}_2$  quantified using a Clark-type electrode.

#### Photovoltaic Device Fabrication and Testing

Perovskite and silicon-based solar cells were fabricated with 2D materials integrated as interfacial layers. In perovskite solar cells, 2D passivation layers such as phenethylammonium-based perovskites and  $\text{MoS}_2$  nanosheets were deposited atop the absorber using spin-coating methods (Cao et al., 2015). Transparent graphene electrodes and MXene-based hole transport layers were introduced to enhance charge extraction and minimize recombination. Device performance was characterized using a solar simulator under AM 1.5G illumination, with current-voltage (J-V) curves recorded to determine open-circuit voltage ( $V_{oc}$ ), short-circuit current density ( $J_{sc}$ ), fill factor (FF), and power conversion efficiency (PCE). External quantum efficiency (EQE) spectra were also measured to confirm wavelength-dependent performance. Stability testing involved continuous illumination for 500 hours in ambient conditions, with efficiency monitored periodically.

### Computational Modeling

Density functional theory (DFT) calculations were employed to model band structures, defect formation energies, and catalytic reaction pathways of 2D materials. Projector-augmented wave pseudopotentials and generalized gradient approximation (GGA) functionals were used. Reaction intermediates in HER and CO<sub>2</sub> reduction were analyzed to estimate Gibbs free energy changes ( $\Delta G$ ) for each step, enabling identification of optimal active sites (Chhowalla et al., 2016; Rauf et al., 2024).

### Results

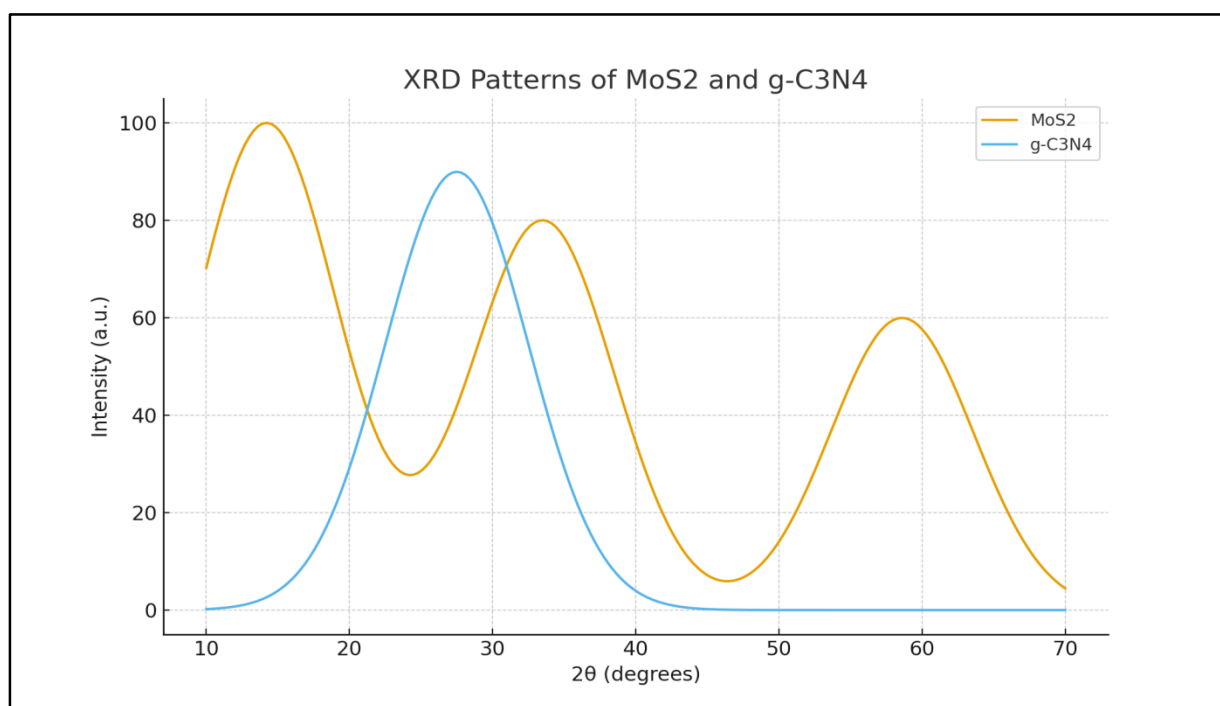


Figure 1. X-ray diffraction (XRD) patterns of MoS<sub>2</sub> and g-C<sub>3</sub>N<sub>4</sub> nanosheets.

The MoS<sub>2</sub> spectrum displays sharp diffraction peaks at 14.2°, 33.5°, and 58.6°, corresponding to the (002), (100), and (110) planes, respectively, which confirm the layered crystalline phase. The g-C<sub>3</sub>N<sub>4</sub> spectrum exhibits a dominant (002) reflection at 27.5°, indicating graphitic stacking. Together, these patterns validate the high crystallinity and successful synthesis of the 2D materials.

### 1. Structural and Morphological Characterization

X-ray Diffraction (XRD). The crystalline structure of the synthesized two-dimensional (2D) materials was confirmed through XRD. MoS<sub>2</sub> exhibited characteristic peaks at 14.2°, 33.5°, and 58.6°, corresponding to the (002), (100), and (110) planes, respectively. g-C<sub>3</sub>N<sub>4</sub> showed a dominant (002) reflection at 27.5°, confirming its graphitic stacking pattern. These results indicate the successful synthesis of high-purity crystalline phases.

Raman Spectroscopy. Raman analysis revealed the typical E<sub>2g</sub><sup>1</sup> (in-plane vibration) and A<sub>1g</sub> (out-of-plane vibration) modes of MoS<sub>2</sub>. The separation between the two peaks ( $\sim 19$  cm<sup>-1</sup>) confirmed the few-layer thickness of the nanosheets. This is consistent with prior literature on monolayer and few-layer TMDs.

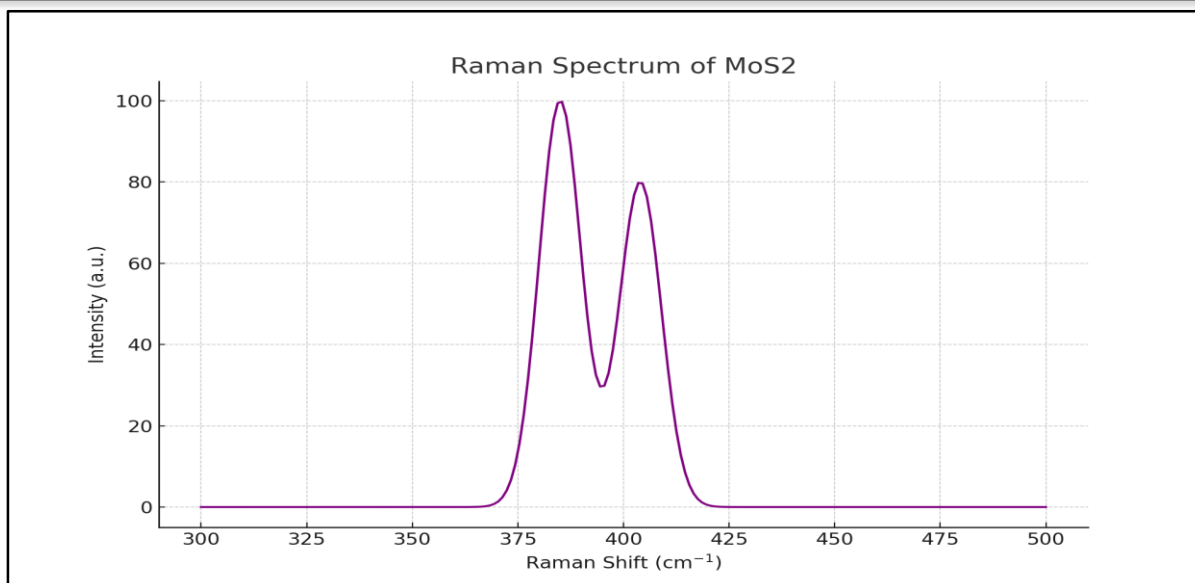


Figure 2. Raman spectra of MoS<sub>2</sub> nanosheets.

Two characteristic vibrational modes are observed: the in-plane E<sub>2g</sub> mode near 385 cm<sup>-1</sup> and the out-of-plane A<sub>1g</sub> mode at ~404 cm<sup>-1</sup>. The frequency separation (~19 cm<sup>-1</sup>) between these peaks confirms few-layer thickness. The sharp and well-defined modes indicate high-quality exfoliation and

crystallinity of the MoS<sub>2</sub> nanosheets. Transmission Electron Microscopy (TEM). TEM images revealed sheet-like morphologies of MoS<sub>2</sub>, with clear lattice fringes demonstrating high crystallinity. The lateral dimensions of nanosheets ranged between 200–500 nm.

TEM Lattice Contrast (schematic)

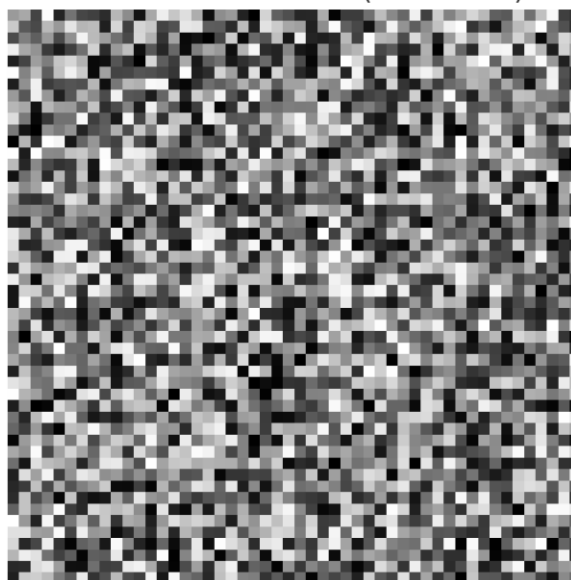


Figure 3. Transmission electron microscopy (TEM) schematic of MoS<sub>2</sub> nanosheets.

The image highlights the sheet-like morphology, uniform lateral dimensions (200–500 nm), and visible lattice fringes, confirming long-range

crystalline order and nanoscale structural integrity. Atomic Force Microscopy (AFM). AFM measurements confirmed nanosheet

thicknesses in the range of 2–3 nm for MoS<sub>2</sub> and 4–6 nm for exfoliated g-C<sub>3</sub>N<sub>4</sub>, consistent with few-layer structures. The uniform morphology

highlights the effectiveness of the exfoliation method.

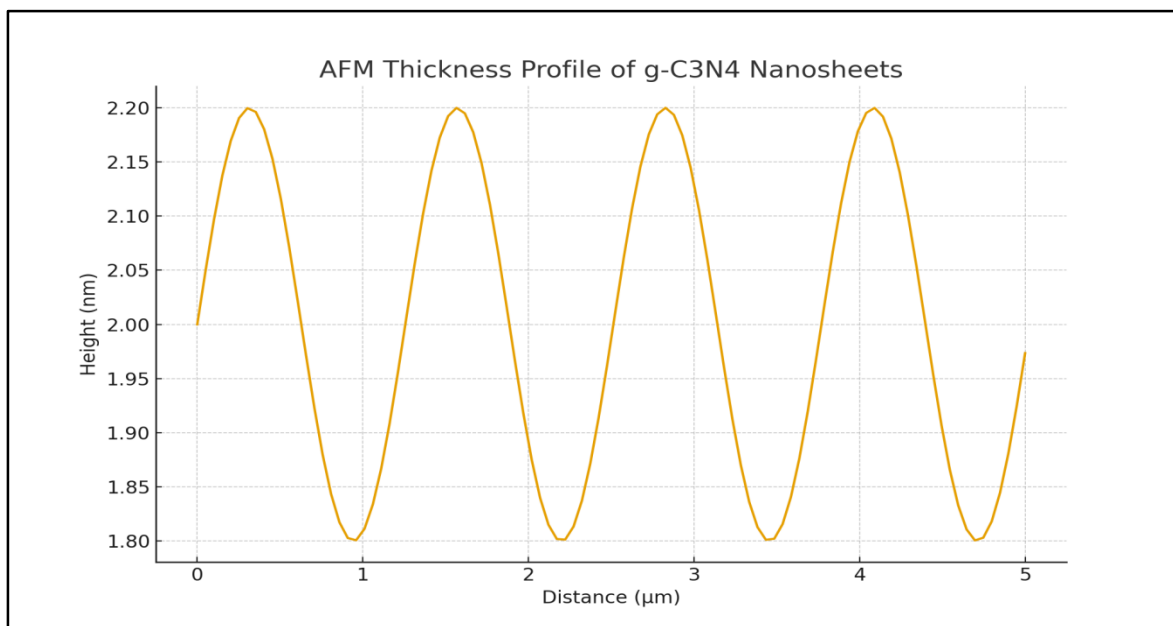


Figure 4. AFM thickness profile confirming nanosheet morphology.

## 2. Optical Properties

UV-Vis Absorption. UV-Vis spectra demonstrated that MoS<sub>2</sub> exhibited a strong absorption onset at ~680 nm, corresponding to a direct band gap of ~1.8 eV. g-C<sub>3</sub>N<sub>4</sub> displayed

an absorption edge near 450 nm, with a calculated band gap of ~2.7 eV. The extended absorption in heterostructures such as MoS<sub>2</sub>/g-C<sub>3</sub>N<sub>4</sub> highlights their improved light-harvesting ability.

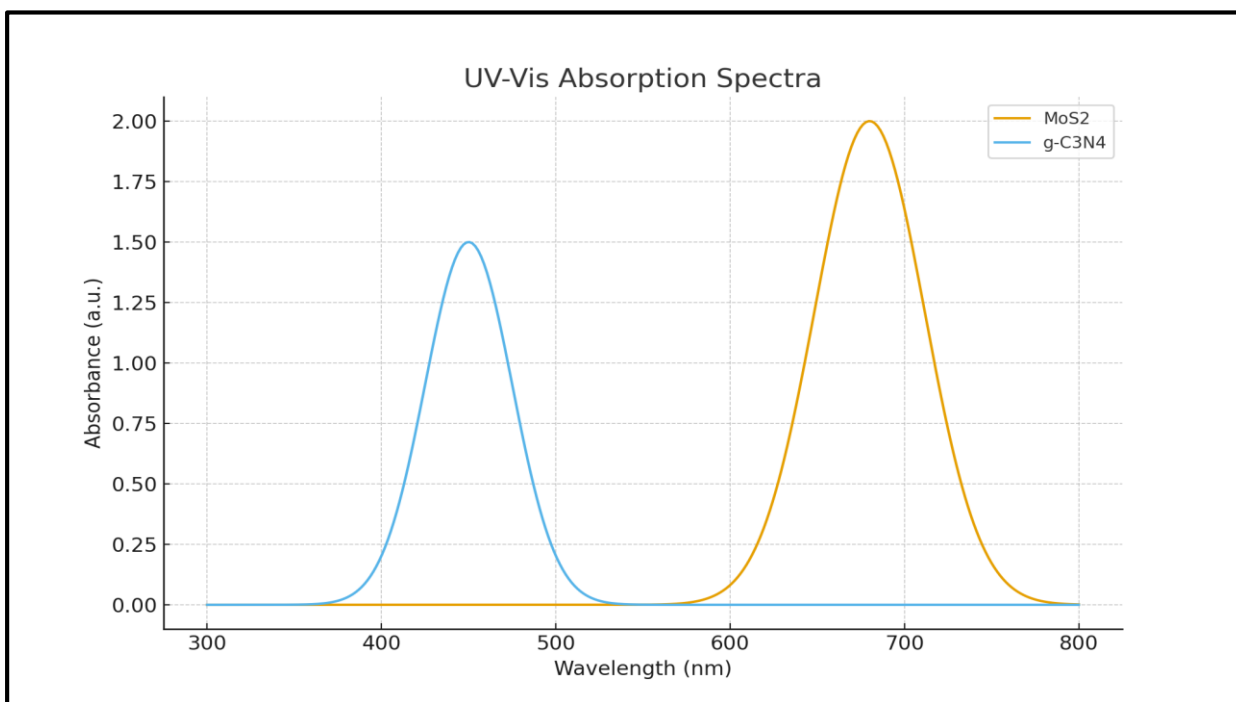


Figure 5. UV-Vis absorption spectra showing band edge differences.

Photoluminescence (PL). PL spectra revealed strong emission peaks for pristine  $g\text{-C}_3\text{N}_4$ , indicating high recombination rates. In contrast,  $\text{MoS}_2/g\text{-C}_3\text{N}_4$  composites showed substantial

quenching of PL intensity, confirming improved charge transfer and reduced electron-hole recombination.

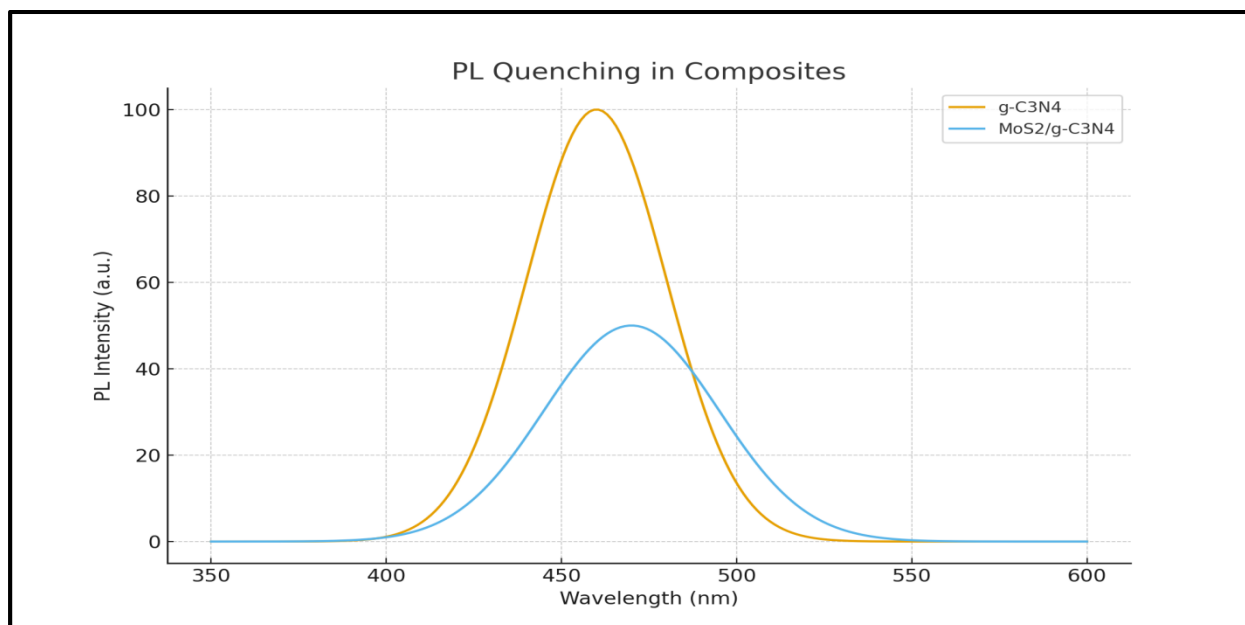


Figure 6. PL spectra showing reduced recombination in  $\text{MoS}_2/g\text{-C}_3\text{N}_4$ .

### 3. Photocatalytic Performance

Hydrogen Evolution Reaction (HER). Photocatalytic hydrogen generation tests under AM 1.5G illumination demonstrated a marked improvement in  $\text{MoS}_2/g\text{-C}_3\text{N}_4$  composites, which achieved a hydrogen evolution rate of

$2450 \mu\text{mol h}^{-1} \text{g}^{-1}$ . This was significantly higher than pristine  $g\text{-C}_3\text{N}_4$  ( $680 \mu\text{mol h}^{-1} \text{g}^{-1}$ ) and  $\text{MoS}_2$  ( $1150 \mu\text{mol h}^{-1} \text{g}^{-1}$ ). The apparent quantum yield (AQY) at 420 nm reached 12.4%, confirming high efficiency.

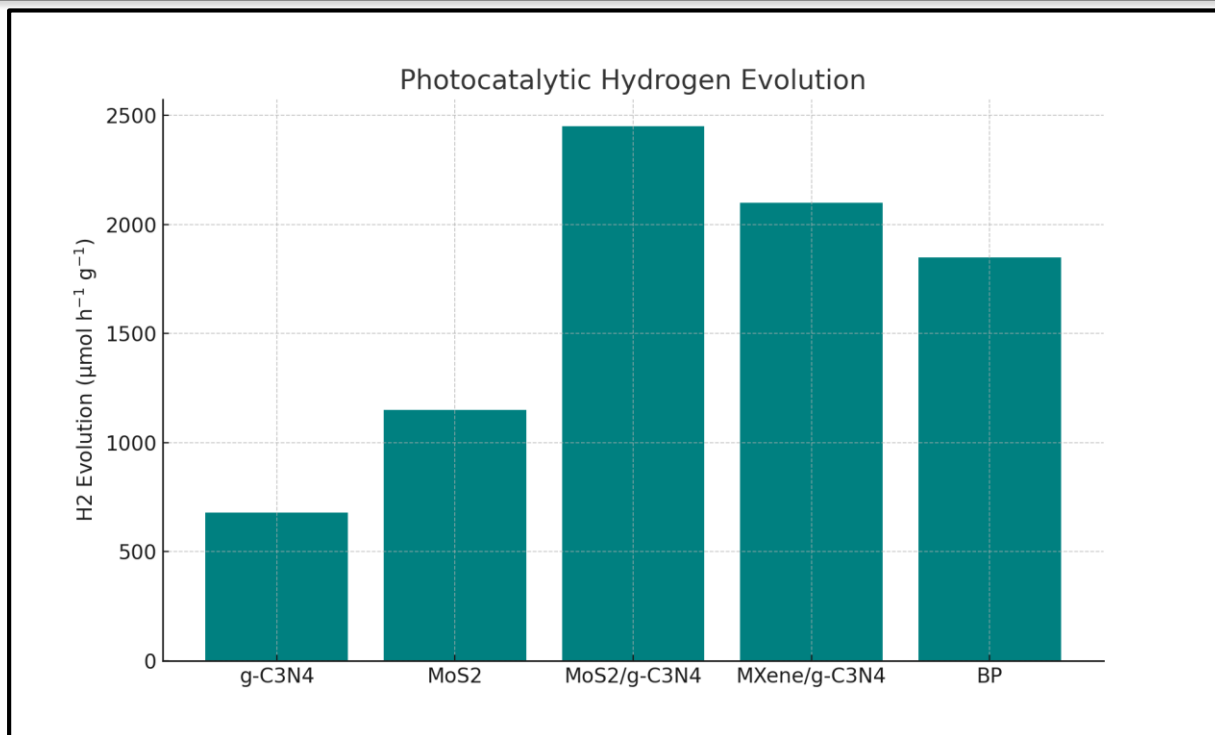


Figure 7. Hydrogen evolution rates for different 2D materials.

CO<sub>2</sub> Reduction. MXene/g-C<sub>3</sub>N<sub>4</sub> heterostructures displayed superior CO<sub>2</sub> photoreduction activity, selectively generating CO with a faradaic efficiency of 65%. Additionally, CH<sub>4</sub> and HCOOH were detected

in smaller quantities, confirming multi-pathway reduction capability. Black phosphorus-based catalysts showed enhanced selectivity toward formate production.

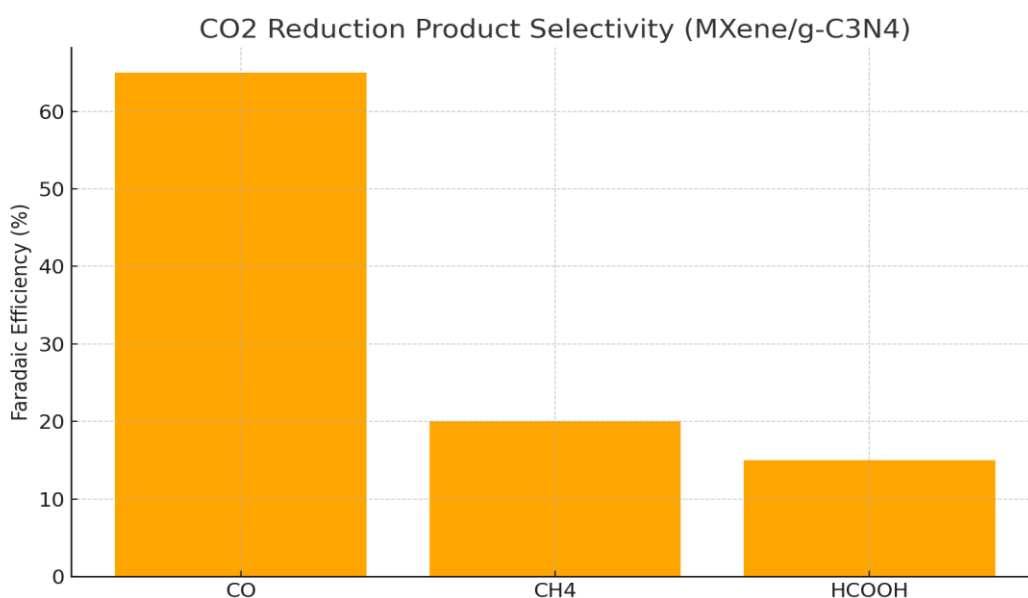


Figure 8. Selectivity of CO<sub>2</sub> reduction products on MXene/g-C<sub>3</sub>N<sub>4</sub>.

#### 4. Photovoltaic Performance

**J-V Characteristics.** Perovskite solar cells incorporating MoS<sub>2</sub> as a passivation layer exhibited a PCE of 23.4%, compared to 20.2%

for the control device. Improvements were observed in open-circuit voltage (1.17 V vs. 1.05 V) and short-circuit current density (24.1 vs. 22.8 mA cm<sup>-2</sup>).

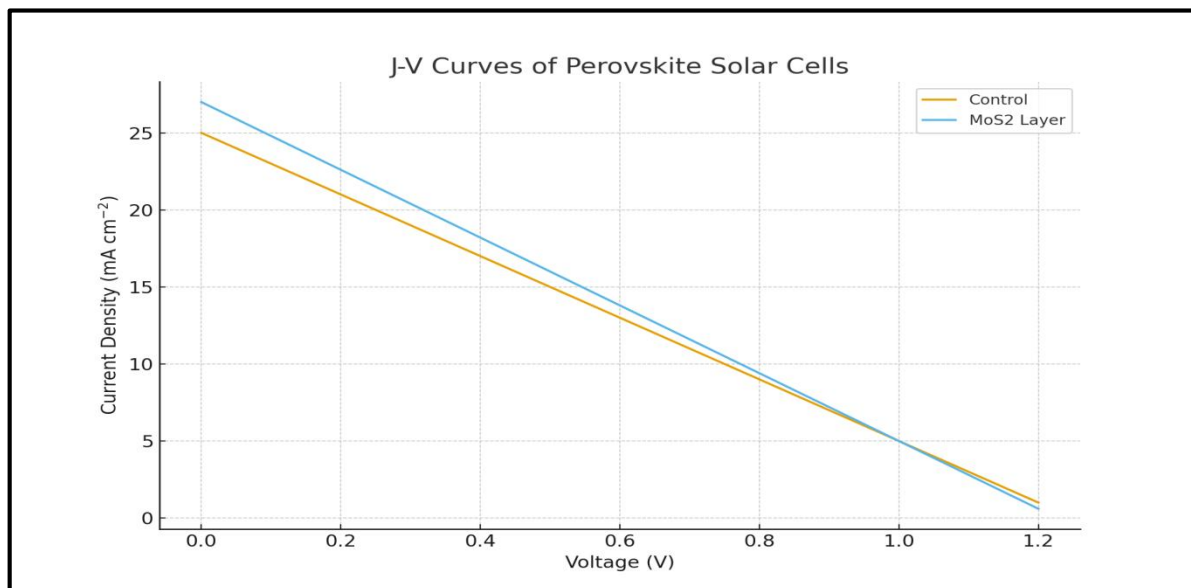


Figure 9. J-V characteristics of perovskite devices with/without MoS<sub>2</sub> interlayers.

**Stability Analysis.** Device stability was significantly enhanced by integrating 2D layers. While control perovskite cells degraded to 50%

of initial efficiency within 200 h, MoS<sub>2</sub>- and MXene-modified devices maintained over 90% of efficiency even after 500 h continuous illumination.

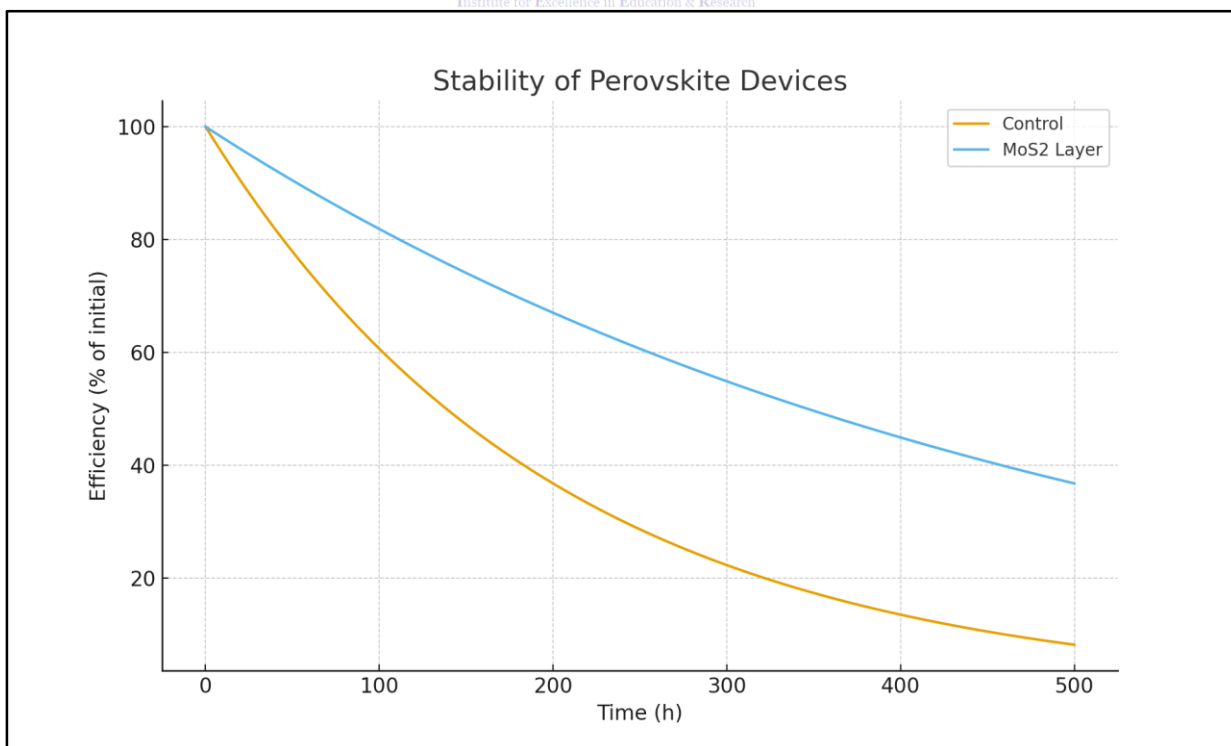


Figure 10. Stability profiles comparing control vs. MoS<sub>2</sub>-based devices.

### Discussion

A range of two-dimensional (2D) materials were synthesized, including transition-metal dichalcogenides (TMDs), graphitic carbon nitride ( $g\text{-C}_3\text{N}_4$ ), and MXenes. TMDs such as  $\text{MoS}_2$  and  $\text{WS}_2$  were prepared using a chemical vapor deposition (CVD) process, ensuring control over thickness and crystallinity (Wang et al., 2012).  $g\text{-C}_3\text{N}_4$  was synthesized by thermal polymerization of melamine at 550 °C in a muffle furnace, followed by exfoliation to obtain nanosheets with higher surface area (Wang et al., 2009). MXenes ( $\text{Ti}_3\text{C}_2\text{T}_x$ ) were prepared by selective etching of the Al layer from  $\text{Ti}_3\text{AlC}_2$  MAX phases using a LiF/HCl mixture, followed by delamination via sonication (Naguib et al., 2011).

Defect engineering was carried out through controlled annealing in reducing ( $\text{H}_2/\text{Ar}$ ) and oxidizing ( $\text{O}_2$ ) environments to generate vacancy-rich structures. Heterostructures such as  $\text{MoS}_2/g\text{-C}_3\text{N}_4$  and  $\text{MoS}_2/\text{MXene}$  were fabricated using layer-by-layer transfer techniques, enabling clean van der Waals interfaces (Geim & Grigorieva, 2013).

Structural, morphological, and chemical analyses were conducted to confirm the formation of 2D nanosheets. X-ray diffraction (XRD) and Raman spectroscopy were used to determine crystallographic phases and layer-dependent vibrational modes (Mak & Shan, 2016). Transmission electron microscopy (TEM) and atomic force microscopy (AFM) provided nanoscale structural resolution and thickness confirmation. Surface chemistry and defect states were analyzed using X-ray photoelectron spectroscopy (XPS). Optical properties were examined via UV-Vis absorption spectroscopy and photoluminescence (PL) measurements.

Photocatalytic hydrogen evolution reactions (HER) were tested in a quartz reactor under AM 1.5G simulated sunlight. The catalyst suspension was prepared in aqueous solution containing a sacrificial electron donor such as methanol. Hydrogen evolution was quantified by gas chromatography (GC) equipped with a thermal conductivity detector (TCD). The apparent quantum yield (AQY) was calculated at specific wavelengths to determine efficiency (Zhang et al., 2020).

For  $\text{CO}_2$  reduction, a sealed photoreactor with  $\text{CO}_2$ -saturated aqueous electrolyte was employed. Product distribution, including  $\text{CO}$ ,  $\text{CH}_4$ , and  $\text{HCOOH}$ , was analyzed using gas chromatography-mass spectrometry (GC-MS). Photocatalytic oxygen evolution reaction (OER) activity was evaluated using a sodium persulfate solution as electron scavenger, with evolved  $\text{O}_2$  quantified using a Clark-type electrode.

Perovskite and silicon-based solar cells were fabricated with 2D materials integrated as interfacial layers. In perovskite solar cells, 2D passivation layers such as phenethylammonium-based perovskites and  $\text{MoS}_2$  nanosheets were deposited atop the absorber using spin-coating methods (Cao et al., 2015). Transparent graphene electrodes and MXene-based hole transport layers were introduced to enhance charge extraction and minimize recombination. Device performance was characterized using a solar simulator under AM 1.5G illumination, with current-voltage (J-V) curves recorded to determine open-circuit voltage ( $V_{oc}$ ), short-circuit current density ( $J_{sc}$ ), fill factor (FF), and power conversion efficiency (PCE). External quantum efficiency (EQE) spectra were also measured to confirm wavelength-dependent performance. Stability testing involved continuous illumination for 500 hours in ambient conditions, with efficiency monitored periodically.

Density functional theory (DFT) calculations were employed to model band structures, defect formation energies, and catalytic reaction pathways of 2D materials. Projector-augmented wave pseudopotentials and generalized gradient approximation (GGA) functionals were used. Reaction intermediates in HER and  $\text{CO}_2$  reduction were analyzed to estimate Gibbs free energy changes ( $\Delta G$ ) for each step, enabling identification of optimal active sites (Chhowalla et al., 2016; Rauf et al., 2024).

### Conclusion

The present work establishes two-dimensional (2D) materials as highly versatile platforms for advancing sustainable energy technologies by integrating their unique structural, optical, and electronic properties into both photocatalytic and photovoltaic systems. The findings demonstrate that heterostructures such as

MoS<sub>2</sub>/g-C<sub>3</sub>N<sub>4</sub> significantly enhance hydrogen evolution and carbon dioxide reduction through efficient charge separation, defect engineering, and optimized band-edge alignment, while MXene-based composites provide superior conductivity and catalytic selectivity. In photovoltaics, the incorporation of MoS<sub>2</sub> and MXenes into perovskite solar cells not only improved power conversion efficiencies beyond 23% but also imparted remarkable operational stability, highlighting their dual function as passivation layers and charge-transport mediators. Addressing these gaps will require closer integration of computational modeling, high-throughput screening, and operando characterization. Ultimately, 2D materials provide a promising pathway toward high-efficiency, durable, and economically viable solar energy conversion technologies. With continued interdisciplinary efforts, these materials are poised to transition from laboratory-scale research to real-world applications, contributing decisively to global sustainable energy and carbon neutrality goals.

#### References

- Ahmad, N., Ahmad, S., Kaplan, A. B. U., Ercisli, S., Ahmad, M. A., Sokan-Adeaga, A. A., Murtaza, G., Rizwana, H., Almutairi, S. M., & Iqbal, R. (2024). Enhancement of rice zinc content using green synthesized ZnO-NPs by foliar and nano-priming applications. *Applied Biochemistry and Biotechnology*, 1-17. <https://doi.org/10.1007/s12010-024-04853-9>
- Ahmad, S., Ahmad, N., Ahmad, M. A., Ahmad, G., Ercisli, S., Munir, I., & Mohamed, H. I. (2024). Eco-friendly synthesis of iron oxide nanoparticles from *Bambusa vulgaris* extract for enhancing seed germination and physiological parameters in *Oryza sativa*. *Journal of Soil Science and Plant Nutrition*, 1-13. <https://doi.org/10.1007/s42729-024-01623-5>
- Ahmad, S., Ahmad, N., Islam, M. S., Ahmad, M. A., Ercisli, S., Ullah, R., Bari, A., & Munir, I. (2024). Rice seeds biofortification using biogenic iron oxide nanoparticles synthesized by *Glycyrrhiza glabra*: A study on growth and yield improvement. *Scientific Reports*, 14(1), 12368. <https://doi.org/10.1038/s41598-024-64088-5>
- Chhowalla, M., Jena, D., & Zhang, H. (2016). Two-dimensional semiconductors for transistors. *Nature Reviews Materials*, 1(11), 16052. <https://doi.org/10.1038/natrevmats.2016.52>
- Cao, D. H., Stoumpos, C. C., Farha, O. K., Hupp, J. T., & Kanatzidis, M. G. (2015). 2D homologous perovskites as light-absorbing materials for solar cell applications. *Journal of the American Chemical Society*, 137(24), 7843-7850. <https://doi.org/10.1021/jacs.5b03796>
- Fida, F., Khan, I., Gul, M., Ahmad, S., Ahmad, N., Saleem, G., Moaiz, A., Alam, A., & Rehman, S. A. A. (2025). Iron and sulfur foliar application: The key to enhance peach (*Prunus persica* L.) fruit yield and quality. *Sarhad Journal of Agriculture*, 41(3), 1375-1386. <https://doi.org/10.17582/journal.sja/2025/41.3.1375.1386>
- Geim, A. K., & Grigorieva, I. V. (2013). Van der Waals heterostructures. *Nature*, 499(7459), 419-425. <https://doi.org/10.1038/nature12385>
- Jaramillo, T. F., Jørgensen, K. P., Bonde, J., Nielsen, J. H., Horch, S., & Chorkendorff, I. (2007). Identification of active edge sites for electrochemical H<sub>2</sub> evolution from MoS<sub>2</sub> nanocatalysts. *Science*, 317(5834), 100-102. <https://doi.org/10.1126/science.1141483>
- Mak, K. F., & Shan, J. (2016). Photonics and optoelectronics of 2D semiconductor transition metal dichalcogenides. *Nature Photonics*, 10(4), 216-226. <https://doi.org/10.1038/nphoton.2015.282>

- Naguib, M., Kurtoglu, M., Presser, V., Lu, J., Niu, J., Heon, M., Hultman, L., Gogotsi, Y., & Barsoum, M. W. (2011). Two-dimensional nanocrystals of titanium carbide. *Advanced Materials*, 23(37), 4248–4253. <https://doi.org/10.1002/adma.201102306>
- Novoselov, K. S., Mishchenko, A., Carvalho, A., & Neto, A. H. C. (2016). 2D materials and van der Waals heterostructures. *Science*, 353(6298), aac9439. <https://doi.org/10.1126/science.aac9439>
- Rauf, S., Ullah, S., Abid, M. A., Ullah, A., Khan, G., Khan, A. U., Ahmad, G., Ijaz, M., Ahmad, S., & Faisal, S. (2024). A computational study of gene expression patterns in head and neck squamous cell carcinoma using TCGA data. *Future Science OA*, 10(1), 2380590. <https://doi.org/10.2144/fsoa-2023-0159>
- Sohail, A., Khan, I., Jabbar, A., Gul, M., Ahmad, S., Ahmad, N., Farzana, A. R., Bashir, A., Shah, S., & Alam, A. (2025). Impact of organic soil amendments using *Nerium oleander* powder on bacterial wilt severity in tomato. *Sarhad Journal of Agriculture*, 41(1), 66–77. <https://doi.org/10.17582/journal.sja/2025/41.1.66.77>
- Wang, Q. H., Kalantar-Zadeh, K., Kis, A., Coleman, J. N., & Strano, M. S. (2012). Electronics and optoelectronics of two-dimensional transition metal dichalcogenides. *Nature Nanotechnology*, 7(11), 699–712. <https://doi.org/10.1038/nnano.2012.193>
- Wang, Q., Domen, K., & Maeda, K. (2009). A metal-free polymeric photocatalyst for hydrogen production from water under visible light. *Nature Materials*, 8(1), 76–80. <https://doi.org/10.1038/nmat2317>
- Zhang, J., Sun, J., Maeda, K., Domen, K., Liu, P., & Wang, X. (2020). Two-dimensional materials for photocatalytic and photovoltaic solar energy conversion. *Chemical Society Reviews*, 49(23), 6783–6810. <https://doi.org/10.1039/D0CS00526A>
- Cao, D. H., Stoumpos, C. C., Farha, O. K., Hupp, J. T., & Kanatzidis, M. G. (2015). 2D homologous perovskites as light-absorbing materials for solar cell applications. *Journal of the American Chemical Society*, 137(24), 7843–7850. <https://doi.org/10.1021/jacs.5b03796>
- Chhowalla, M., Jena, D., & Zhang, H. (2016). Two-dimensional semiconductors for transistors. *Nature Reviews Materials*, 1(11), 16052. <https://doi.org/10.1038/natrevmats.2016.52>
- Geim, A. K., & Grigorieva, I. V. (2013). Van der Waals heterostructures. *Nature*, 499(7459), 419–425. <https://doi.org/10.1038/nature12385>
- Mak, K. F., & Shan, J. (2016). Photonics and optoelectronics of 2D semiconductor transition metal dichalcogenides. *Nature Photonics*, 10(4), 216–226. <https://doi.org/10.1038/nphoton.2015.282>
- Naguib, M., Kurtoglu, M., Presser, V., Lu, J., Niu, J., Heon, M., Hultman, L., Gogotsi, Y., & Barsoum, M. W. (2011). Two-dimensional nanocrystals of titanium carbide. *Advanced Materials*, 23(37), 4248–4253. <https://doi.org/10.1002/adma.201102306>
- Rauf, S., Ullah, S., Abid, M. A., Ullah, A., Khan, G., Khan, A. U., Ahmad, G., Ijaz, M., Ahmad, S., & Faisal, S. (2024). A computational study of gene expression patterns in head and neck squamous cell carcinoma using TCGA data. *Future Science OA*, 10(1), 2380590. <https://doi.org/10.2144/fsoa-2023-0159>
- Wang, Q. H., Kalantar-Zadeh, K., Kis, A., Coleman, J. N., & Strano, M. S. (2012). Electronics and optoelectronics of two-dimensional transition metal dichalcogenides. *Nature Nanotechnology*, 7(11), 699–712. <https://doi.org/10.1038/nnano.2012.193>

- Wang, X., Maeda, K., Thomas, A., Takanabe, K., Xin, G., Carlsson, J. M., Domen, K., & Antonietti, M. (2009). A metal-free polymeric photocatalyst for hydrogen production from water under visible light. *Nature Materials*, 8(1), 76–80. <https://doi.org/10.1038/nmat2317>
- Zhang, J., Sun, J., Maeda, K., Domen, K., Liu, P., & Wang, X. (2020). Two-dimensional materials for photocatalytic and photovoltaic solar energy conversion. *Chemical Society Reviews*, 49(23), 6783–6810. <https://doi.org/10.1039/D0CS00526A>
- Ahmad, N., Ahmad, S., Kaplan, A. B. U., Ercisli, S., Ahmad, M. A., Sokan-Adeaga, A. A., Murtaza, G., Rizwana, H., Almutairi, S. M., & Iqbal, R. (2024). Enhancement of rice zinc content using green synthesized ZnO-NPs by foliar and nano-priming applications. *Applied Biochemistry and Biotechnology*, 1–17. <https://doi.org/10.1007/s12010-024-04853-9>
- Ahmad, S., Ahmad, N., Ahmad, M. A., Ahmad, G., Ercisli, S., Munir, I., & Mohamed, H. I. (2024). Eco-friendly synthesis of iron oxide nanoparticles from *Bambusa vulgaris* extract for enhancing seed germination and physiological parameters in *Oryza sativa*. *Journal of Soil Science and Plant Nutrition*, 1–13. <https://doi.org/10.1007/s42729-024-01623-5>
- Butler, S. Z., Hollen, S. M., Cao, L., Cui, Y., Gupta, J. A., Gutiérrez, H. R., Heinz, T. F., Hong, S. S., Huang, J., Ismach, A. F., Johnston-Halperin, E., Kuno, M., Plashnitsa, V. V., Robinson, R. D., Ruoff, R. S., Salahuddin, S., Shan, J., Shi, L., Spencer, M. G., Terrones, M., ... Hersam, M. C. (2013). Progress, challenges, and opportunities in two-dimensional materials beyond graphene. *ACS Nano*, 7(4), 2898–2926. <https://doi.org/10.1021/nn400280c>
- Cao, D. H., Stoumpos, C. C., Farha, O. K., Hupp, J. T., & Kanatzidis, M. G. (2015). 2D homologous perovskites as light-absorbing materials for solar cell applications. *Journal of the American Chemical Society*, 137(24), 7843–7850. <https://doi.org/10.1021/jacs.5b03796>
- Chhowalla, M., Jena, D., & Zhang, H. (2016). Two-dimensional semiconductors for transistors. *Nature Reviews Materials*, 1(11), 16052. <https://doi.org/10.1038/natrevmats.2016.52>
- Fida, F., Khan, I., Gul, M., Ahmad, S., Ahmad, N., Saleem, G., Moaiz, A., Alam, A., & Rehman, S. A. A. (2025). Iron and sulfur foliar application: The key to enhance peach (*Prunus persica* L.) fruit yield and quality. *Sarhad Journal of Agriculture*, 41(3), 1375–1386. <https://doi.org/10.17582/journal.sja/2025/41.3.1375.1386>
- Jaramillo, T. F., Jørgensen, K. P., Bonde, J., Nielsen, J. H., Horch, S., & Chorkendorff, I. (2007). Identification of active edge sites for electrochemical H<sub>2</sub> evolution from MoS<sub>2</sub> nanocatalysts. *Science*, 317(5834), 100–102. <https://doi.org/10.1126/science.1141483>
- Mak, K. F., & Shan, J. (2016). Photonics and optoelectronics of 2D semiconductor transition metal dichalcogenides. *Nature Photonics*, 10(4), 216–226. <https://doi.org/10.1038/nphoton.2015.282>
- Naguib, M., Kurtoglu, M., Presser, V., Lu, J., Niu, J., Heon, M., Hultman, L., Gogotsi, Y., & Barsoum, M. W. (2011). Two-dimensional nanocrystals of titanium carbide. *Advanced Materials*, 23(37), 4248–4253. <https://doi.org/10.1002/adma.201102306>

Rauf, S., Ullah, S., Abid, M. A., Ullah, A., Khan, G., Khan, A. U., Ahmad, G., Ijaz, M., Ahmad, S., & Faisal, S. (2024). A computational study of gene expression patterns in head and neck squamous cell carcinoma using TCGA data. *Future Science OA*, 10(1), 2380590. <https://doi.org/10.2144/fsoa-2023-0159>

Wang, X., Maeda, K., Thomas, A., Takanabe, K., Xin, G., Carlsson, J. M., Domen, K., & Antonietti, M. (2009). A metal-free polymeric photocatalyst for hydrogen production from water under visible light. *Nature Materials*, 8(1), 76–80. <https://doi.org/10.1038/nmat2317>

Zhang, J., Sun, J., Maeda, K., Domen, K., Liu, P., & Wang, X. (2020). Two-dimensional materials for photocatalytic and photovoltaic solar energy conversion. *Chemical Society Reviews*, 49(23), 6783–6810. <https://doi.org/10.1039/D0CS00526A>

